BULETINUL INSTITUTULUI POLITEHNIC DIN IAŞI
Publicat de
Universitatea Tehnică „Gheorghe Asachi” din Iaşi
Volumul 71 (75), Numărul 2, 2025
Secţia
CONSTRUCŢII DE MAŞINI
DOI: 10.2478/bipcm-2025-0015

INFLUENCE OF STRESS CONCENTRATORS ON TENSILE SPECIMENS

BY

GABRIEL-MĂDĂLIN MURARU and CIPRIAN-IONUȚ MORĂRAȘ*

“Gheorghe Asachi” Technical University of Iași,
Faculty of Mechanical Engineering, Iași, Romania

Received: May 6, 2025
Accepted for publication: June 5, 2025

Abstract. Stress concentrators play a crucial role in the mechanical behaviour of tensile specimens, significantly influencing their strength, deformation and failure mode. This study investigates the effects on the stress concentrator on the stress distribution and fracture characteristics of steel specimens subjected to tensile testing. Three specimens were subjected to tensile tests. Electrical resistive tensometry was used to determine the material characteristics.

Keywords: tensile test, strain gauge concentrator shape.

1. Introduction

Tension concentrators, such as notches, holes, and sharp geometrical transitions, significantly affect the mechanical behaviour of materials under tensile loading. These discontinuities create localized stress amplification, leading to premature failure and reducing the overall strength of the component.

---

*Corresponding author; *e-mail*: ciprian-ionut moraras@academic.tuiasi.ro

Understanding the influence of stress concentration is essential in designing mechanical structures, as it directly impacts material performance, fatigue life, and failure resistance (Pilkey and Pilkey, 2008).

Stress concentration factors (SCF) are commonly used to quantify the increase in local stress around discontinuities. Experimental and numerical studies have demonstrated that SCF depend on the geometry, size, and distribution of these discontinuities (Neuber, 1958). Advanced techniques such as finite element analysis (FEA) provide accurate predictions of stress distribution and failure initiation points, complementing traditional analytical methods (Radaj and Vormwald, 2013; Layth al-Kisswani, 2023).

Various materials, including metals, polymers, and composites, exhibit different responses to stress concentrators. For ductile materials, stress redistribution and plastic deformation can delay failure, whereas brittle materials tend to fracture suddenly at stress concentration sites (Anderson, 2005). Understanding these behaviours allows engineers to optimize designs and improve structural integrity in aerospace, automotive, and civil engineering applications.

In case of static loading, the presence of stress concentrators leads to a plastic deformation at their base and to a reduction of the local stress, for structural components made of materials with ductile behaviour. Thus, the critical stress at failure, defined as the global nominal stress, will be higher for a component with a stress concentrator than for a smooth component having the same net cross-section, which exhibits a strong bottleneck before failure. In contrast, for materials with brittle behaviour, this phenomenon does not occur, as there is a high sensitivity to the presence of stress concentrators. Thus, in general, the strength of a smooth component will be higher, (Negru, 2009; Goanta, 2014).

The presence of stress concentrators is also important in determining the duration of life at various stresses in both ductile and brittle materials. From the data published in the technical literature on the fatigue resistance of smooth components and with voltage concentrators respectively for different constant amplitude levels, it appears that the fatigue resistance in the presence of concentrators accounts for an increasing percentage of the resistance of smooth components as the nominal stress level increases (Stephens, 2001).

2. Materials and Methods

In this paper, tensile tests were performed according to ISO EN 6892:2010, on three cylindrical specimens made of a 0.45% carbon quality carbon steel (OLC 45). Figure 1a shows the geometry of specimen one with a diameter of 8 mm over the calibration length. Figure 1b shows the geometry of specimen two, on which a stress concentrator with a diameter of 7 mm. Figure 1c shows specimen three, with a diameter of 10 mm over the calibration length, which is in accordance with the standard ISO EN 6892:2010.

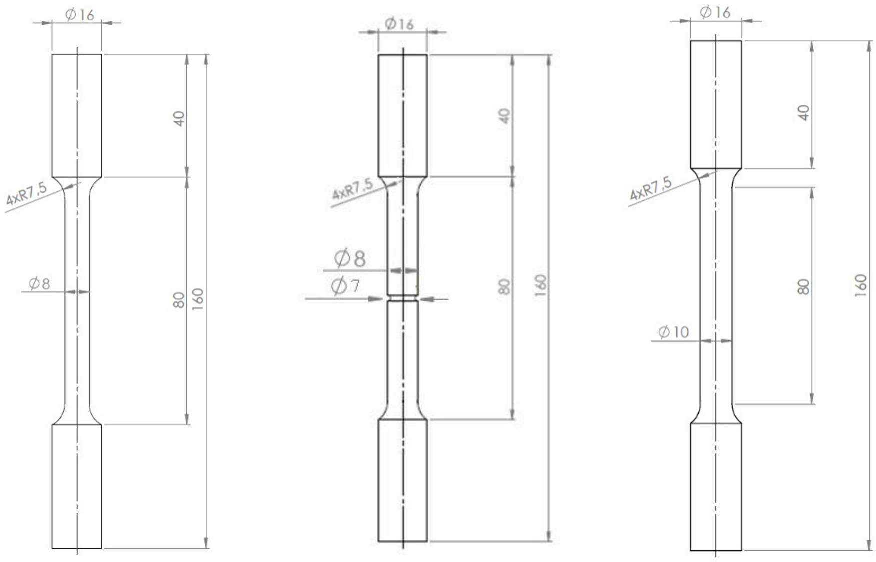

a) b) c)

Fig. 1 – Designs and dimensions of specimens.

In order to determine the mechanical characteristics, the tests on the three specimens, Figure 2(a, b, c), were carried out at room temperature on the WDW 50 universal machine, which is driven by the AD800 automatic measuring system. The maximum force of the machine is 50 KN. The test regime was determined by the rate of strain increase at 2 mm/min for each specimen until failure.

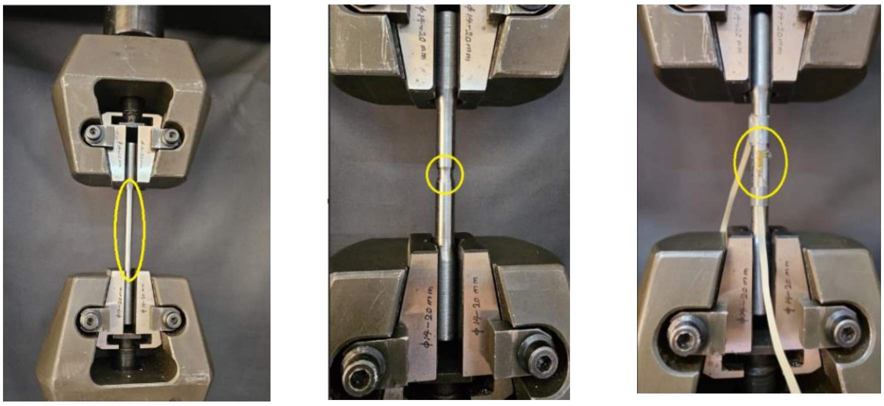

a) b) c)

Fig. 2 – WDW 50 testing machine and specimen set.

In order to determine the elastic characteristics of the material, E, G and ν, two strain gauge, oriented at 0° which will provide a ε_L, and 90° which will provide a ε_T, oriented with respect to the test direction, were placed on the third specimen Fig. 2c. The strain gauges are EA-13-249LZ-120, made by VISHAY (USA), with resistance R=120Ω±0.35%, mark factor k_G=2.095±0.5% and transverse sensitivity K_t=0.2%. In both cases, the cables were connected, with Vishay P3 bridge, in quarter bridge connection. The deformations obtained after load application were read on the bridge screen and the experimental results were recorded for further processing. Strains and deformations are determined by:

$$\sigma = \frac{N}{A};\ E=\frac{\sigma}{\varepsilon_L};\ \nu = \frac{\varepsilon_{Tr}}{\varepsilon_L};\ G=\frac{E}{2(1+\nu)} \qquad (1)$$

where σ= normal stress *N*=axial effort; *A*=transvers section area; E= Young's modulus; ε_L= longitudinal deformation; ε_{Tr} = transverse deformation; G= shear modulus; ν= Poisson's ratio.

3. Results and Discussion

Figure 3 shows the stress-strain characteristic curve for the specimen one that was subjected to tensile stress with a calibration length of $L_0 = 80$ mm and a diameter $d_0 = 8$ mm. After failure the length increased $L_u = 86.43$ mm, and the diameter decreased $d_u = 5.3$ mm. Analyzing the appearance of the stress-strain characteristic curve, a slow failure of the material is observed, with significant deformation between the flow and rupture phases, storing a large amount of strain energy. These aspects are predominant in ductile materials. It can be seen from the characteristic curve that the ultimate tensile stress $\sigma_{UTS} = 571.65$ MPa. Figure 4 shows the two fracture surfaces of the specimen. From the appearance and shape of the surface we have a ductile fracture, due to the cup-cone fracture shape. There is a central depth (cup) and a prominence (cone) on the other side of the fracture. At the macrostructural level there is a fibrous, irregular and mat surface.

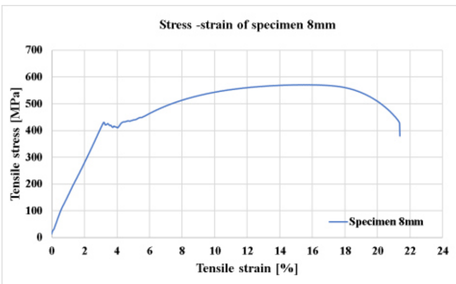

Fig. 3 – Stress-strain diagram of specimen of $d_0 = 8$ mm.

Fig. 4 – Typical ductile fracture appearance for OLC45 steel.

Figure 5 shows the stress-strain characteristic curve for the specimen two that was subjected to tensile stress, with the stress concentrator in the middle. This specimen had an initial calibration length.$L_0 = 80$ mm and a diameter $d_0 = 8$ mm. After failure the length increased $L_u = 80.41$ mm, and the diameter decreased $d_u = 5.73$ mm. Analyzing the appearance of the stress-strain characteristic curve, one observes a sudden failure of the material that exhibits minor plastic deformation and stores a small quantity of strain energy. These aspects are predominant in brittle materials. It can be seen from the characteristic curve that the ultimate tensile stress $\sigma_{UTS} = 696.65$ MPa. Figure 6 illustrates the two fracture surfaces of the specimen. From the appearance and shape of the surface we have a brittle fracture, due to the stress concentrator, the edges are at 45 degrees, with no signs of stretching or great elongation. At the macrostructural level there is a crystalline or granular aspect specific to this type of failure.

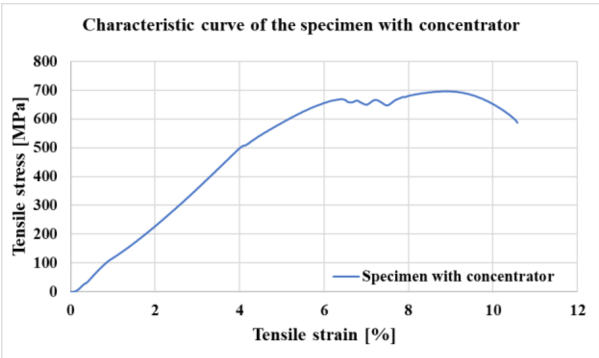

Fig. 5 – Stress-strain diagram for stress concentrator specimen.

Fig. 6 – Typical brittle fracture appearance for OLC45 steel.

Figure 7 shows the stress-strain characteristic curve for the specimen three. Before testing, it had a length $L_0 = 80$ mm and a diameter $d_0 = 10$ mm. After failure the length increased $L_u = 88.49$ mm, and the diameter decreased $d_u = 6.29$ mm. It can be seen from the characteristic curve that the ultimate tensile stress $\sigma_{UTS} = 538.98$ MPa. In Figure 8, from the surface appearance and shape we have a ductile fracture, identical to Figure 4.

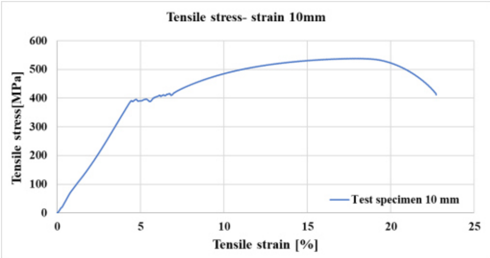

Fig. 7 – Stress strain diagram of specimen d_0 =10 mm.

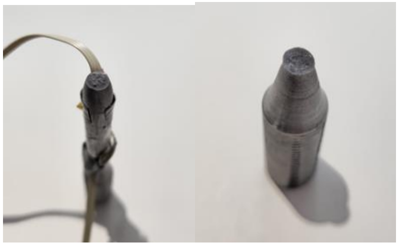

Fig. 8 – Typical ductile fracture appearance for OLC45 steel.

Figure 9 presents the normal stress (σ) / longitudinal specific strain (ε_L) coordinate plots of the longitudinal modulus of elasticity, E, (Young's modulus) for the specimens of diameter $d_0 = 10$ mm. The Young's modulus was determined as the slope of the line of approximation of the graph plotted in the coordinates normal stress (σ) / longitudinal specific strain (ε_L), through the points determined from the records of the force values by the WDW 50 machine calculator and the longitudinal specific strains.

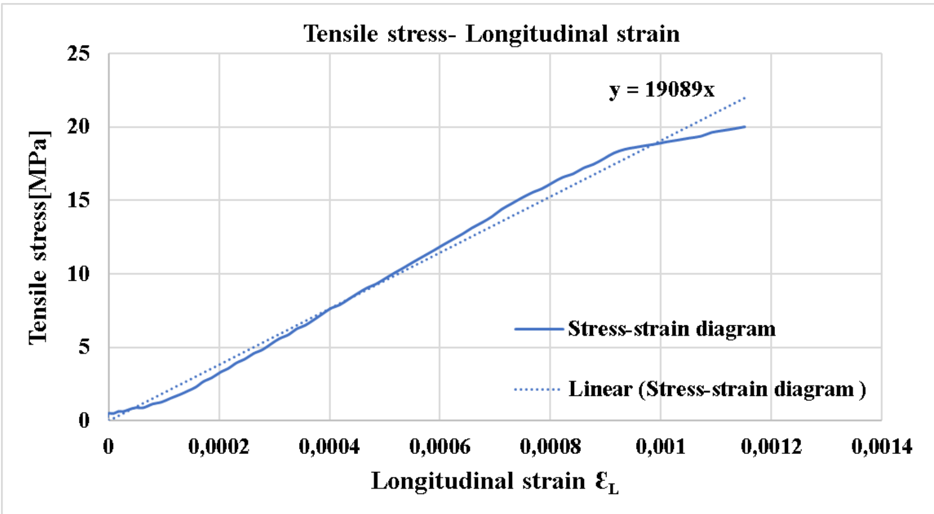

Fig. 9 – Stress variation with longitudinal strain-approximation line for Young's modulus determination.

In Figure 10, plots in the coordinates of transverse specific strain (ε_T) / longitudinal specific strain (ε_L) for determining the Poisson's ratio ν. The slope of the approximation line represents the coefficient of transverse Poisson's shrinkage. Following the determination of the Young's modulus, the Poisson's ratio and relation (1), G= 7575 MPa.

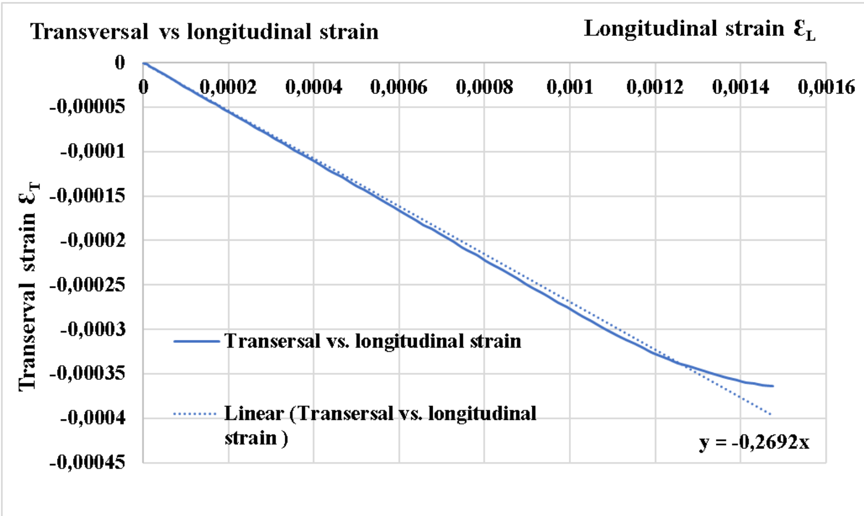

Fig. 10 – Longitudinal strain-transversal strain curve.

Following the experimental determinations, the strength and deformability characteristics were determined, table 1, using equation:

- *percentage elongation after fracture* A:

$$A = \frac{L_u - L_0}{L_0} * 100 \quad (2)$$

- percent reduction of the area Z:

$$Z = \frac{S_0 - S_u}{S_0} * 100 \quad (3)$$

- *Yield strength:*

$$\sigma_c = \frac{F_c}{S_0} \quad (4)$$

- *tensile strength:*

$$\sigma_r = \frac{F_{max}}{S_0} \quad (5)$$

Table 1
Calculation results

	A [%]	Z [%]	σ_c[MPa]	σ_r[MPa]
Specimen one	8.03	56.11	437.9	604.1
Specimen two	0.51	48.7	696.66	716.56
Specimen three	10.61	60.44	439.5	573.25

4. Conclusions

In this paper, a study on the influence of stress concentrator on tensile test behavior was carried out. It was found that after tensile testing, the deformability characteristics of specimens with a stress concentrator significantly varied compared to specimens without a stress concentrator. The maximum stresses and strains are localized in the area of the stress concentrator. The specimen failed at the stress concentrator before the total elongation of the specimen achieved the value of the specimen with geometry 1. In the case of specimen three, the tensile strength is lower, having a value of 573.25 MPa, compared to specimen one due to the volume of material that specimen three has, and consequently there are more microstructural defects in the material. The obtained results demonstrate a homogeneous and isotropic behavior of the material.

REFERENCES

Anderson T.L., *Fracture Mechanics: Fundamentals and Applications*, CRC Press (2005).

Goanta V., *The influence of the fatigue cycles number on material hardness*, Applied Mechanics and Materials (2014).

Layth AL-K., Fayez, S., Goanță V., *Designing to minimize the influence of stress concentrators*, Bul. Inst. Polit. Iaşi, DOI:10.2478/bipcm-2023-0003.

Negru R.M., *Contribuţii la studiul efectului de concentrare a tensiunilor cu aplicaţii în mecanica ruperii şi oboseala materialelor*, Timișoara (2009).

Neuber H., *Theory of Stress Concentration for Shear-Strained Prismatical Bodies with Arbitrary Nonlinear Stress-Strain Law*, Journal of Applied Mechanics, 28(4), 544-550 (1961).

Pilkey W.D., Pilkey D.F., *Peterson's Stress Concentration Factors*, Wiley (2008).

Radaj D., Vormwald M., *Advanced Methods of Fatigue Assessment*, Springer (2013).

Stephens R.I., *Metal Fatigue in Engineering*, New York: 2nd edition, John Wiley & Sons, Retrieved from Anderson Materials Evaluation, Inc (2001).

INFLUENȚA CONCENTRATORILOR DE TENSIUNE ASUPRA EPRUVETELOR SUPUSE LA TRACȚIUNE

(Rezumat)

Concentratorii de tensiuni joacă un rol crucial în comportamentul mecanic asupra probelor supuse la tracțiune, influențând semnificativ rezistența, deformarea și modul de rupere al acestora. Acest studiu investighează efectele concentratorului de tensiuni asupra distribuției tensiunilor și a caracteristicilor de rupere ale epruvetelor din oțel. Trei epruvete au fost supuse la încercarea de tracțiune statică. În scopul determinarii constantelor elastice de material s-a utilizat tensometria electrică rezistivă.